Ecological Modelling
May 2020, Volume 423 Pages 109006 (14p.)
https://doi.org/10.1016/j.ecolmodel.2020.109006
https://archimer.ifremer.fr/doc/00613/72469/

Impact of environmental variability on *Pinctada margaritifera* life-history traits: A full life cycle deb modeling approach

Sangare Nathanaël [1, *], Lo-Yat Alain [1], Le Moullac Gilles [1], Pecquerie Laure [2], Thomas Yoann [2], Lefebvre Sebastien [3], Le Gendre Romain [4], Beliaeff Benoit [1], Andréfouët Serge [5]

[1] Ifremer, UMR Ecosystèmes Insulaires Océaniens, UPF, ILM, IRD, Taravao, F-98719, Tahiti, French Polynesia
[2] Univ Brest, CNRS, IRD, Ifremer, LEMAR, F-29280 Plouzane, France
[3] Université de Lille, CNRS, ULCO, UMR 8187 LOG, F-62930 Wimereux, France
[4] IFREMER, LEAD NC, Nouméa, New Caledonia
[5] UMR 9220 ENTROPIE, Institut de Recherche Pour le Développement, (IRD,Université de la Réunion, Université de la Nouvelle-Calédonie, Ifremer, CNRS), B.P.A5, 98848 Nouméa, New Caledonia

* Corresponding author : Nathanaël Sangare, email address : nathanael.sangare@ifremer.fr

Abstract :

The black-lipped pearl oyster (*Pinctada margaritifera*) is extensively farmed in French Polynesia to produce black pearls. For a sustainable management of marine resources, studying interactions between organisms and environment, and the associated factors and processes that will impact their life cycle and thus modulate population dynamics is a major research priority. Here, we describe black-lipped pearl oyster energy acquisition and use, and its control by temperature and food concentration within the Dynamic Energy Budget (DEB) theory framework. The model parametrization was based on literature data and a specific laboratory experiment. Model validation was carried out thanks to historical in-situ datasets and a dedicated field survey. Three theoretical environmental scenarios were built to investigate the response of the pearl oyster to environmental variations. We successfully modeled a wide range of life-stage-specific traits and processes, especially the delayed acceleration of growth after settlement. Applying the model on field data collected at three different culture sites required only one free-fitted parameter, the half saturation coefficient Xk, which controls how ingestion depends on food density. Xk integrates all variations linked to the trophic environment. Analysis of the kinetics of energy fluxes under theoretical environmental scenarios suggests that temperature variations induce seasonality of reproduction in a species thought to spawn opportunistically throughout the whole year. The major influence of food concentration fluctuations on growth rate and reproductive effort is highlighted. The model showed the lower performances associated with recovery time between food-rich and starvation periods. The implications of these findings in the context of black pearl farming in a changing environment are discussed.

Highlights

► DEB theory was successfully applied to the full life cycle of *P. margaritifera* ► The model captures life-history traits variability in contrasted environmental conditions ► Environmental fluctuations significantly impact oyster's performances ► Temperature variations tend to drive reproduction seasonality ► Duration of starvation periods drives annual reproductive effort

Keywords : Bivalve, Physiology, Bioenergetics, Dynamic energy budget theory, Environmental change, Pearl farming

Introduction

In French Polynesia, pearl production is based on the culture of a single species: the black-lipped pearl oyster (*Pinctada margaritifera,* Linnaeus, 1758) (Andréfouët et al., 2012), a suspension-feeding bivalve living in the oligotrophic waters of atoll lagoons and coral reefs. Pearl oyster aquaculture takes place mostly in atoll lagoons, and has a major economic and social function since it employs about 1500 workers in remote atolls and represents the second income of the territory behind tourism (ISPF, 2016). Supply of juvenile oysters to farmers is largely dependent on the natural collection of larvae on artificial substrates and spat collecting variability and effectiveness impact the pearl industry. At the lagoon scale, spatio-temporal spat collection variability depends on the multiple factors that drive reproduction, larval development and recruitment success.

Tropical atolls lagoons are often described as stable and homogenous environments, with high temperature and low biomass of the different planktonic communities and with small seasonal variations (e.g. Charpy et al., 1997; Dufour et al., 1999; Torréton and Dufour, 1996). Behind this apparent stability, French Polynesian atoll lagoons experience spatial and temporal variations of temperature and food availability at both intra and inter-lagoon scales according to seasons and geographical positions (Charpy et al., 1997; Lefebvre et al., 2012; Thomas et al., 2010). Previous studies (Fournier et al., 2012b; Thomas et al., 2012) suggested that these environmental variations impact oyster's life history traits such as the reproduction efficiency and pelagic larval duration, which are two key life steps for spat collection success. However, in these remote exploited ecosystems, the influence of these local environmental conditions on this oyster's life history, and ultimately on black-pearl farming sustainability, has remained poorly studied so far.

Besides the individual differences of metabolic process inherent to the oyster, such as nutrition capacity, growth or reproduction rates (Long KY and Le Moullac,

2017), the growth and development of the pearl oyster depend on complex interactions between physiology, environmental conditions and food availability (e.g. Chávez-Villalba et al., 2013; Doroudi et al., 1999; Pouvreau et al., 2000b). To quantify the consequences of environmental variability on *P. margaritifera* physiology, Fournier, (2011) and Thomas et al., (2011) built two distinct Dynamic Energy Budget (DEB) models for the adult and the larval stages respectively. At that time, the most suitable method for parameter estimation (van der Meer, 2006) constrained the authors to partially calibrate their models based on *Crassostrea gigas* parameters. These models have shown their ability to realistically simulate various physiological processes, and thus have laid a solid foundation for a comprehensive understanding of the factors underlying pearl oyster sensitivity to environmental fluctuations, such as recruitment variations in space and time (Thomas et al., 2016a). However, an integrative model for the full *P. margaritifera* life cycle, able to describe continuously growth, reproduction, larval development and recruitment potential was still missing. As the sustainable management of marine resources relies on the estimation of the species' current and future sizes, fitness, abundances and distributions, a full life cycle model is critical to model future population dynamics and the influence of changes in environmental factors.

DEB theory (Kooijman, 2010) offers a framework that describes the metabolic organization underlying the physiological functions of an organism in a fluctuating environment. Based on a restricted number of assumptions, written out as mathematical formulas, this theory allows the description of growth, development and reproduction throughout an organism's life cycle, as a function of available food and temperature. Its application is challenging because the state variables and parameters are abstract quantities that are not directly observable. Recent developments allow estimating all parameters of a DEB model using standard empirical datasets (Marques et al., 2018). Such calibrated DEB models have already been useful to predict the effects of global change, and better understand species geographical patterns, environmental stressors effects, bio-production optimization and management of exploited resources (e.g. Desforges et al., 2017; Molnár et al., 2011; Muller et al., 2019).

Here, DEB theory was applied to assess the pearl oyster's life cycle sensitivity to the spatial and temporal variations of temperature and food, with a particular emphasis on growth, reproduction, and larval development. The parameters were estimated using a wide range of datasets provided by the literature and supplemented by a specific laboratory experiment (Sangare et al., 2019). The model was then

validated using data specifically acquired for this study, as well as independent historical *in situ* data from three contrasted environments. Finally, a sensitivity analysis was performed to investigate how life history traits can vary within a wide range of environmental conditions known to occur (or that may potentially occur) in French Polynesian atoll lagoons. The implications in the context of black pearl farming are discussed.

Material and methods

An approach combining *in situ* monitoring, laboratory experiment and modelling (with observation, calibration, validation and application), was used for our objectives. We provide here a short overview of our method before developing it in the next sections. A recent development, specifically "the AmP project", was used to fully calibrate the model (Marques et al., 2018). A field survey took place in the lagoon of Ahe (Tuamotu, French Polynesia) where oyster's reproduction, growth and environmental data were monitored simultaneously. The collected data were used jointly with literature data to validate the model ability to describe oyster's life history traits in three contrasted environments across the French Polynesian latitudes (Ahe, Takapoto and Gambier). Then, scenarios of food and temperature fluctuations were implemented to investigate the theoretical pearl oyster's response to environmental variations. These steps are detailed below.

Study site

The Ahe atoll is located at 14°29'S–146°18'W, 500 km Northeast of Tahiti Island in the northern Tuamotu Archipelago (Figure 1). Ahe lagoon is a 142 km^2 semi-enclosed atoll with a mean depth close to 42 m and a lagoon-wide e-flushing time of approximately 80-days (Dumas et al., 2012). The only active deep pass is located in the north western part of the lagoon and several shallow reef-flat spillways (less than 50 cm depth) are distributed along the reef rim, mainly on the south facing side of the rim. Ahe is a pilot site for pearl farming research program since 15 years (Andréfouët et al., 2012) as it hosts an important pearl farming activity. The atoll already benefits from a 3D hydrodynamical model (Dumas et al., 2012) which was extensively used for larval dispersal investigations (Thomas et al., 2016a).

145 Field work: adult growth, reproduction and environment data in Ahe atoll

146 Chlorophyll a (chl-a) concentration, as a proxy for food availability, and
147 temperature were monitored during a six months field survey (February to August
148 2017) at 2 different sampling stations (Figure 1) assumed to be environmentally
149 contrasted (Thomas et al., 2012). All measuring devices were placed at a depth of 5
150 m, directly on the rearing lines where the animals sampled were attached (see below).
151 Temperature was recorded every 4 hours by iBcode22L temperature sensor. Food
152 conditions were monitored hourly by two multi-parameter SMATCH® probes during
153 four sampling periods: 02/24/2017 - 03/13/2017; 04/10/2017 - 04/19/2017; 05/26/2017
154 - 06/05/2017 and 07/02/2017 - 08/15/2017.

155 SMATCH® probes measurements accuracy was controlled by comparing with
156 direct measurement of chl-a every 6 weeks. Water samples (500 ml) were taken and
157 filtered on GF/F Whatman filters (ca. 0.7 µm pore size). Chl-a was extracted from
158 phytoplankton cells during 8h in the dark in 6 ml of ethanol 70%. Concentration of chl-
159 a was then quantified by chl-a fluorescence determined using a Trilogy® fluorimeter
160 calibrated with chl-a standard (Sigma) and equipped with the appropriates optical
161 filters (Welschmeyer, 1994).

162 Three cohorts of oysters per sampling site were used to monitor growth and
163 reproductive effort. In the first two ones, 2 groups of 30 oysters, with initial average
164 lengths equal to 9.5 ± 1 cm (mean ± standard deviation) and 12 ± 1 cm were monitored
165 for growth measurement. Four measurements were performed at the beginning of
166 each of the aforementioned sampling period. The measurement of shell length (Hynd,
167 1955) was carried out according to a conservative method of individual labeling. For
168 the third cohort, a total of 1440 *P. margaritifera* at the adult stage (mean size = 11 ± 1
169 cm) was divided on 48 batches of 30 individuals, and 24 batches were placed at each
170 station on rearing lines. The measurement of the reproductive effort was weekly
171 recorded at each station during 6 months. Every 7 days, at each station, from February
172 to August 2017, the Gonado-Digital Index (*GDI*, %) was measured on 30 individuals.
173 *GDI* measurements were obtained by image analysis of the sagittal section of the
174 gonado-visceral mass (image processing on Adobe® Photoshop® CS3 then analysis
175 by ImageJ® 1.51j8). A description of the present sampling schemes and methods are
176 also detailed in Fournier et al., (2012). Finally, for comparison with DEB model outputs,
177 the *GDI*, which is a surface area ratio, was converted to a Gameto-Somatic Index
178 (*GamSI*, %), which is a mass ratio between reproduction buffer and flesh weight.
179 Assuming no relative differences in weights between the components of the gonado-

visceral mass, the following relationship was used to calculate *GamSI* from field data:

$$GamSI = \frac{GDI \cdot W_{w\_visc}}{W_w} \quad (1)$$

where W_{w_visc} is the wet weight of the visceral mass and W_w the total flesh wet weight.

Model description

To describe the growth, development and reproduction of *P.* margaritifera as a function of temperature and food conditions, we developed a bioenergetic model, which relies on the concepts of DEB theory (Kooijman, 2010) (Figure 2 and see Appendix A for the general description and equations of the different fluxes). The model revisits with new data and parameterization design (Marques et al., 2018) the works of Thomas et al., (2011) and Fournier, (2011) who applied the standard DEB model to *P. margaritifera* at the larval and adult stage respectively. Our objective was to obtain a single set of parameters, with some stage-specific ones, to represent the full life cycle of *P. margaritifera*.

According to the DEB models previously developed for bivalves (Bourlès et al., 2009) in case of starvation, the maintenance costs were prioritized over reproduction then growth if needed. When the mobilized reserve does not cover all maintenances costs, the reproduction buffer takes over. Note that no lysis of the structure was allowed in our model, hence the individual dies if the reserve and the reproduction buffer cannot cover maintenance costs.

Spawning is triggered according to an opportunistic strategy (Le Moullac et al., 2012; Pouvreau et al., 2000a, 2000c), regardless of the environmental conditions i.e. no food nor temperature threshold are required for spawning. When *GamSI,* the ratio between the gonadic and total dry flesh mass (see Eq. 7 below), reaches a given threshold ($GamSI_{Threshold}$) a part of the reproduction buffer is released. The parameter "*SpawnRatio*" defines this amount of stored energy, which is released at each spawn. According to Fournier, (2011) and our own unpublished data of *GamSI* and histological analysis for 40 individuals right after spawning triggered by thermal choc, 80% of the spawners had a *GamSI* close to 0.15, while the other 20% totally emptied their stored gonad products.

The DEB model presented here specifies the complete life cycle of *P. margaritifera*. It is of the *asj* type which takes into account the delayed acceleration of

growth rate that is reported by Sangare et al. (2019) to occur right after settlement. The model assumed isomorphy except between the settlement and juvenile stage, where metabolism accelerates following the rules for V1-morphy (Kooijman, 2014) until the oyster reaches the juvenile stage. The consequence is that growth is not only accelerated by a larger intake, but also by a larger mobilization from reserve in comparison to an isomorph. Under this assumption, values of surface-area-specific assimilation rate ($\{p_{Am}\}$) and energy conductance ($\dot{v}$) after the metamorphosis depend on the feeding history during the larval stage, which may partly explain the natural variability in parameters between individuals of the same species (Kooijman et al., 2011). This phase is called type *M* acceleration (s_M) and we refer the reader to Kooijman (2014) for a detailed description.

The egg energy content E_0 is fixed from calculations made by Acosta-Salmón (2004). Stage transitions occur at defined thresholds of the cumulated energy into maturation E_H (Figure 3). An embryo becomes a larva at $E_H = E_H^b$, settles and metamorphoses (changes its shape) at $E_H = E_H^s$, reaches juvenile stage (without change in morphology) at $E_H = E_H^j$, and matures into an adult at $E_H = E_H^p$. Metabolic acceleration occurs from settlement until juvenile stage. In addition, the model incorporates one shape coefficient for the adult (δ_M) and a different one for the larvae ($\delta_{M.larv}$) since larvae morphometry changes at settlement (Southgate and Lucas, 2011).

Finally, the full model of the temperature correction was used with high and low boundaries of the optimal temperature range being specified and parameterized (see Appendix A & B). A simpler form (with one parameter) is often used in DEB studies when solely temperature conditions within the optimal range are considered. This is the case in the older version of the DEB model for *P. margaritifera* (Fournier, 2011) and most bivalves studies with the exception of Thomas et al. (2011). Throughout the manuscript, all rates are given at the reference temperature of 20°C (= 293.15 K).

Link between DEB state variables and observable quantities

State variables of DEB models can be related to quantities typically used in aquaculture science or ecophysiological experiments, specifically: shell length, body dry weight and batch fecundity, using auxiliary equations. Shell length L_w (cm) (Hynd, 1955) is computed from the structural volume V (cm^3) and the shape coefficient δ_M or $\delta_{M\ larv}$ according to the maturity stage:

$$L_w = \frac{V^{1/3}}{\delta_M} \quad (2)$$

The flesh dry weight (W_d, g) is the sum of the dry weight of structure W_V, reserve W_E and reproduction buffer W_{ER} that can be defined as:

$$W_V = d_V \cdot V \quad (3)$$

$$W_E = \frac{w_E}{\mu_E} \cdot E \quad (4)$$

$$W_{ER} = \frac{w_E}{\mu_E} \cdot E_R \quad (5)$$

$$W_d = W_V + W_E + W_{ER} \quad (6)$$

with d_V the specific (dry) density of structure (g cm^3), w_E the reserve specific dry weight (g mol^{-1}) and μ_E the reserve chemical potential (J mol^{-1}).

The gameto-somatic index (*GamSI*, %) is then computed using the following formula:

$$GamSI = \frac{W_{ER}}{W_d} \quad (7)$$

Model parameters estimation

The "AmP" procedure was applied with MATLAB® (R2017b) to infer the DEB model parameters (Marques et al., 2018). This method uses experimental and field observations at different life stages and calibrates the parameters thanks to a Nelder-Mead numerical optimization that minimizes the difference between observed and predicted values, based on a weighted least-squares criterion. Initial values of the parameters were set following Thomas et al., (2011) and Fournier, (2011). Thirty datasets from the literature were used for model calibration ranging from length or age at different life stages, to respiration rate at different conditions of food and temperature (Sangare et al., 2019). The list of input data extracted from the literature is available at (Nathanael Sangare. 2019. *AmP Pinctada margaritifera*, version 2019/05/06): https://www.bio.vu.nl/thb/deb/deblab/add_my_pet/entries_web/Pinctada_margaritifera/Pinctada_margaritifera_res.html

The parameter X_k, a component of the law governing ingestion, is the only parameter of the *P. margaritifera*-DEB model that can be tuned freely for further

applications in contrasting environments (Alunno-Bruscia et al., 2011; Fournier et al., 2012a; Thomas et al., 2011) This environment-specific coefficient reflects the variability in oyster food, and specifically the quantitative and qualitative effects of inorganic material and phytoplankton species on the feeding response of *P. margaritifera.* In this way, the simulation of oyster growth in different Pacific tropical ecosystems is possible with a single set of parameters, with X_k, as the only free-fitting parameter.

Model validation

To assess the accuracy of the model simulations and its generalization to other French Polynesian atoll lagoons, modelled description of the pearl oyster life cycle was tested on four in situ datasets of growth and reproduction at different life stages and in contrasted environments (Table 1). These datasets were all independent from those used for model parametrization.

The data from lot 3, allowed to test the model ability to describe pearl oyster performances at different life stage and latitudes and longitudes far from the pilot site of Ahe, since Gambier island is located by 23°S. Conversely, Tapakoto atoll is only 115 km away from Ahe.

Validation simulations were run in the conditions of food and temperature that were monitored simultaneously, along with the respective biological dataset. The parameter X_K was readjusted for each atoll according to the description of the food conditions and/or the age of the oysters. Several missing values of chl-a concentration during the 2017 Ahe study (Dataset 4) were filled using Fourier series (Curve fitting Toolbox 3.5.6 Copyright 2001-2017 The MathWorks, Inc.) fitted on the chl-a data available at each station.

To account for the inter-individual variability of the validation datasets 2, 3 & 4, the DEB model was applied using a multi-individual-based modelling strategy. The initial individual conditions of the simulations were computed according to the real oyster's length and flesh weights measured individually on each sampled oyster at the first sampling point of each dataset. Individual simulations were performed and then pooled together to compute average patterns.

The agreement between field observations and model simulations was evaluated by linear regression between the samples' mean value of observations (X) and the mean value of individual simulations (Y), which was tested against the Y=X

model at the alpha error threshold of 5%. The R^2 coefficient of determination allowed us to evaluate how much of the variance was explained by the model.

Sensitivity analysis to environmental conditions

The sensitivity of the pearl oyster life history traits to environmental conditions was assessed with three theoretical environmental scenarios taking into account a wide range of temperatures and food concentrations that occur in tropical atoll lagoons, especially in French Polynesia. The effect of temperature on *P. margaritifera* growth and reproduction was investigated within the range 23 to 34 °C. This range brackets the French Polynesia typical seasonal variations, ranging from 27 to 30 °C in the northern Tuamotu Archipelago and 23.5 to 28.5 °C in the Gambier islands (Le Moullac et al., 2012; Pouvreau et al., 2000), and also includes temperature maxima observed during El Niño events (Andréfouët et al., 2018). The effects of food availability on *P. margaritifera* growth and reproduction were investigated within the range 0.05 to 1 $\mu g_{Chl\text{-}a}\ l^{-1}$. In French Polynesian atoll lagoon, chl-a concentrations range from 0.1 to 0.7 $\mu g_{Chl\text{-}a}\ l^{-1}$ with extreme values of 0.05 $\mu g_{Chl\text{-}a}\ l^{-1}$ in the open ocean and 1.2 $\mu g_{Chl\text{-}a}\ l^{-1}$ in Mataiva atoll (Andréfouët et al., 2001; Delesalle and Sournia, 1992). Independently of the atoll mean annual concentration, important variations of the planktonic ecosystem may occur at different time-scales and have been mostly related to grazing pressure (Delesalle et al., 2001; Fournier, 2011; Sakka et al., 1999; Thomas et al., 2010). Basic spectral analysis ("Fast Fourier transform" function from MATLAB® R2107b) on food concentrations time series provided by the 4 validation datasets (see above) were performed, for further representation of food variations.

Thereby, three theoretical scenarios were performed:

1) The influence of temperature and food concentrations were assessed by comparing oysters' life history traits in constant environmental conditions ranging from 0.05 to 1 $\mu g_{Chl\text{-}a}\ l^{-1}$ for food and 23 to 34°C for temperature.

2) The effect of yearly seasonal temperature variations on life history traits was investigated using sinusoid functions (period = 365 days) with a total amplitude ranging from 2 to 8°C and that oscillated around several values ranging from 22 to 35°C. Minimum and maximum temperatures occurred respectively in the middle of austral winter and summer. Here, the food concentration was fixed, and set at the average value of 0.2 $\mu g_{Chl\text{-}a}\ l^{-1}$ based on observations by Charpy et al. (1997) from 16 Tuamotu atoll lagoons.

3) The influence of phytoplankton biomass variations was investigated by considering oscillations around the reference values of 0.1; 0.2 and 0.3 $\mu g_{Chl\text{-}a}\ l^{-1}$ at a mean temperature of 28.5 °C (Charpy et al., 1997; Fournier, 2011; Thomas et al., 2010). Amplitude variations were set to vary from 0.1 to 1 $\mu g_{Chl\text{-}a}\ l^{-1}$. Note that the minimum values were set to 0.01 $\mu g_{Chl\text{-}a}\ l^{-1}$ to keep realistic the dynamic equilibrium of the grazer/phytoplankton system. The phytoplankton biomass turnover rate was investigated by setting the oscillation periods from once a year, to two days.

Simulations were first performed with the values for X_k calibrated in laboratory on larvae and adults feeding on cultivated micro-algae *Isochrysis lutea* and *Chaetoceros gracilis* (Table 2). This assumption does not represent the real variability of food quality and/or appetence of the oysters when considering total chl-a measurements (Alunno-Bruscia et al., 2011). Thus, simulations 1 and 2 were also performed with the values for X_k adjusted during *in situ* model validation.

Life history traits of interest were set according to the constraints inherent to spat collection and pearl production. Namely, these are 1) the reproductive effort within a year for a 13 cm-shell length individual initialized with an empty reproduction buffer at day 0, 2) the pelagic larval duration (PLD) that begin at gamete released and end when the maturity threshold $E_H = E_H^s$ is reached and 3) the time needed to reach commercial size, established at 9 cm, size at which grafting can be performed (Grand and Hauti, 1993).

Results

Parameterization

Parameters values are summarized in Table 2. The overall fit of the AmP method resulted in a mean absolute relative error (MRE) of 0.273 and a mean squared error (SMSE) of 0.294. In general, the calibrated model accurately described the calibration datasets and reproduced well many observations such as growth, filtering or respiration rates, and length/weight ratio reported in the field and laboratory experiments. It also successfully captured the acceleration of growth rate at juvenile stage. The complete set of table and graphics that compared simulation vs. calibration data are available at (Nathanael Sangare. 2019. *AmP Pinctada margaritifera*, version 2019/05/06) :

https://www.bio.vu.nl/thb/deb/deblab/add_my_pet/entries_web/Pinctada_margaritifera/Pinctada_margaritifera_res.html

During the model parameterization, the scaled functional response was assumed to be equal to 0.3 and 0.1 for *in situ* data representing the austral summer and winter respectively. The functional response for the *ad libitum* experimental data sets was set to 0.9 instead of the possible maximum $f = 1$ because it was rather unclear how optimal the nutritional value of the cultivated phytoplankton used for the rearing was for the needs of the animals.

Model validation

Dataset 1

In the case of larval rearing with cultured algae (Figure 4 A), the value of the half-saturation coefficient, X_k, corresponded to that calibrated for larvae experimentally: 0.6 $\mu g_{Chl\text{-}a}\ l^{-1}$ (Table 2). For *in situ* rearing, not supplied with cultured algae (Figure 4 B, C and D), the half-saturation parameter was calibrated at 0.2 $\mu g_{Chl\text{-}a}\ l^{-1}$ to obtain a better fit between simulations and observations. Despite a slight underestimation of the growth rate after day 11 for the rearing in mesocosm (Figure 4 C), the simulation fits were highly significant, with R^2 equal to 0.995; 0.937; 0.943 0.967 respectively for the simulations A, B, C and D with p-values < 0.0001.

Dataset 2

Simulations compared with the validation dataset 2 are presented in Figure 5. Here, the half saturation coefficients were adjusted at 0.7 mg POM l^{-1} for the age group 1 and 0.5 mg POM l^{-1} for age group 2 and 3 to obtain better fits. This way R^2 were equal to 0.864 and 0.884 respectively for the age group 1 and 2 with p-values < 0.0001 and simulations for age group 3 gave an R^2 equal to 0.373 with a p-value of 0.015. Pouvreau et al., (2000a) suggested from their study respectively 1, 2 and 4 spawning events for the age group 1, 2 and 3 represented by blue arrows on the Figure 5. These conclusions are not confirmed by the new simulations that suggested for each age group one spawning event per individual during the year of survey (marked by drops in the thin lines on Figure 5). Individuals spawned continuously during several months (Figure 5 : braces) from August to January for the age groups 1 and 3 (Figure 5 A & C) and from mid-September to mid-January for the age group 2 (Figure 5 B). In any case, 80% or more of the spawning events occurred between mid-September and mid-December.

Dataset 3

Simulations of shell length and dry flesh mass evolution in Gambier Islands are compared with the validation dataset 3 in Figure 6. Here, the value of the half-saturation coefficient, X_k, was readjusted at 0.1 $\mu g_{Chl\text{-}a}\ l^{-1}$ to improve the fits. The simulations usually remained in the range of the observed values except for the large underestimation of the flesh dry mass between February and May (Figure 6 A; R^2 = 0.561; p-value = 0.0277) and an overestimation of the shell length from June to August (Figure 6 B; R^2 = 0.904; p-value = 0.001). Le Moullac et al., (2012) suggested 3 spawning events (Figure 6 blue arrows) in December, March and June. Here, these conclusions are not confirmed by the simulations that suggested one spawn per individual occurring asynchronously throughout the year (sharp decrease in the thin lines).

Dataset 4

Environmental conditions from stations 1 & 3 (Figure 1), are shown Figure 7 A & B respectively. Time-series of gameto-somatic index variations are plotted on Figure 7 C & D. No readjustment of X_k from the value calibrated in laboratory (X_k = 0.2 $\mu g_{Chl\text{-}a}\ l^{-1}$) were needed to obtain better fits. A steady decrease of temperature from about 30 to 27 °C was recorded during the period of observation (February to August or the middle of the austral summer and winter respectively). According to the observations, food concentration and biological measurements did not show clearly defined seasonal variations. Peaks of chl-a concentration happened occasionally during the year. Gametogenesis occurred when food availability allowed it and spawning took place asynchronously the whole year (Figure 7). No massive spawning event could be clearly identified during the field survey.

Here, the model did not accurately reproduce *GamSI* variations, with R^2 equals to 0.057 and 0.125 and p-value equals to 0.1841 and 0.1679 respectively to the Figure 7 C & D. However, the mean value remained relevant within the general range of fluctuations, and clusters of asynchronous spawns occurred when observed *GamSI* decreased (Figure 7 arrows). Note that a slight decrease of *GamSI* occurred at station 3 between mid-April and mid-May without associated spawning events. According to the model simulations, this decrease was due to a low food concentration which led the organisms to pay maintenance costs from the reproduction buffer. Individuals simulated at the station 1 were able to reproduce once or twice depending on the initial

conditions of their gonads, while individuals from station 3 spawned only once during the simulation.

The model accurately described shell growth at different ages and contrasted location within the lagoon of Ahe (Figure 8) with R^2 very close to 0.99 and p-value <0.0001. Since individual shell length values and dynamics were very close to each other, only the mean values of the observed and simulated data are plotted for the sake of clarity.

Sensitivity analysis to environmental conditions

Generally, the model predicted low oysters' performances at low temperature and food, and improved physiological performances with rising conditions until the temperature reached 34.5°C (Figure 9 & Appendix B) after which degrading performances prevented oysters long term survival.

Simulation 1: sensitivity to mean environmental values

Simulation 1 assessed the influence of constant food and temperature levels set at their mean values. Half saturation coefficients were set to 0.2 and 0.6 $\mu g_{Chl\text{-}a}\ l^{-1}$ for adults and larvae respectively. The temperature from 24 to 30°C and food availability from 0.1 to 0.9 µg Chl-a l^{-1} is represented by rectangles on the Figure 9 to highlight the range of French Polynesian atoll lagoon conditions (Delesalle and Sournia, 1992). Within these ranges, we predicted a possible theoretic PLD from 10 to 70 days (Figure 9 A), 2 to 14 spawning events a year for a 13 cm shell length oyster (Figure 9 B) and a commercial size was reached at 12 to 40 months after egg fertilization (Figure 9 C).

According to the dataset 2, Gambier Islands experienced annually a mean food of 0.19 $\mu g_{Chl\text{-}a}\ l^{-1}$, a mean temperature of 25.5 °C and a half saturation coefficient (X_k) suitable for validation equal to 0.1 $\mu g_{Chl\text{-}a}\ l^{-1}$. In these conditions a 13 cm shell length oyster would be able to spawn six times a year and the fertilized eggs would reach a commercial size after 23 months (not shown). Up north, in Ahe atoll, the dataset 4 framed food and temperature at 0.21 $\mu g_{Chl\text{-}a}\ l^{-1}$ and 28.5 °C respectively with a X_k equal to 0.2 $\mu g_{Chl\text{-}a}\ l^{-1}$. Thus, a 13 cm shell length oyster could reproduce 5 times a year and fertilized eggs would reach a commercial size after 24 months.

Similarly, for the value of X_k = 0.2 $\mu g_{Chl\text{-}a}\ l^{-1}$ which was reported *in situ* for larvae in Ahe (Dataset 1), PLD would range between10 to 20 days in the northern Tuamotu archipelago (not shown) when respectively released in austral summer (30°C) and winter (27 °C). No larvae datasets were available to assess X_k in Gambier Island, thus under the assumption that the half saturation coefficient does not differ between locations, the PLD in Gambier would range from 17 to 27 days depending on whether spawning occurred in the summer (28.5 °C) or winter (23.5 °C).

Simulation 2: sensitivity to seasonal temperature variations

Simulation 2 informs on how the seasonal temperature variations affect the growth and reproductive effort of oysters, with simulations performed at constant food levels (0.2 $\mu g_{Chl\text{-}a}\ l^{-1}$), but at various mean temperatures and amplitude variations Figure 10. Seasonal changes occurred at a slow time-scale that did not influence larval development, which is more sensitive to the relative variations at the time of development (see Figure 9 A). Seasonal amplitudes affected oysters' growth and reproduction differently depending on the average annual temperature. For instance, for a mean temperature value of 26 °C, no effect of the seasonal variations was reported on growth or reproduction, but at 29 °C the time to reach commercial size slowed to 5 months and reproduction effort was divided by 1.5 along the gradient of temperature amplitude (Figure 10). According to the actual range of temperature conditions occurring in French Polynesia (Figure 10: rectangles), oysters needed from 23 to 26 months to reach a commercial size (Figure 10 A) and spawners of 13 cm shell length could reproduce 4 to 5 times a year (Figure 10 B).

A mean fluctuation of 2 to 3 °C occur in the northern Tuamotu Archipelago where the mean annual temperature comes close to 28.5 °C; whereas a mean variation of 5 to 6 °C for an average annual temperature of 25.5 °C is recorded in the Gambier Islands. Then, using X_k values suitable (see above) for Ahe atoll and Gambier islands, it appeared that oysters needed 23 months to reach a commercial size, while spawners can reproduce 5 times a year in any case.

Seasonal fluctuations of temperatures introduced seasonality of reproductive outputs. For a mean annual temperature of 28 °C and seasonal amplitude greater than 4 °C, three of the five spawning events reported by the simulations occurred when temperature is above 28 °C. On the other hand, reproduction occurred at more regular

intervals over the year when the temperature difference between austral summer and winter is below 4 °C.

Simulation 3: sensitivity to phytoplankton biomass stability

The preliminary spectral analysis of the environmental conditions of the validation datasets (datasets 1; 2; 3 and 4) did not reveal any periodic signal in food variations (not shown). The absence of a regular time interval between food-rich and starvation periods suggested that fluctuation can be approximated by random variation in the field.

Here, only results for oscillations that ranged from 0.1 to 1 $\mu g_{Chl\text{-}a}\ l^{-1}$ around the reference value of 0.2 $\mu g_{Chl\text{-}a}\ l^{-1}$ are represented. Changing the reference food concentration had qualitatively no impact on the general pattern of the life history traits. Indeed, the shape of the isoclines would just be redrawn around the horizontal line defined by the chosen reference value (Figure 11, dotted lines = reference value of 0.2 $\mu g_{Chl\text{-}a}\ l^{-1}$).

The amplitude of food variations was related to the total amount of food available for oysters and a food variation lower than the reference value reflected stable food conditions over time (below 0.2 $\mu g_{Chl\text{-}a}\ l^{-1}$: Figure 11 dotted lines). Below this reference, oysters' energy management induced small growth variations (Figure 11 A) and reproductive efforts (Figure 11 B). Within these limits the time required to reach commercial size varied from 23 to 26 months and the yearly number of spawns varied from 3 to 5 events. Conversely, if the cycle amplitude was greater than the reference value for food, variations of life history traits became mainly driven by the oscillation period.

Oscillation period was related to alternating plentiful and starvation phases. At high cycle amplitudes (above 0.2 $\mu g_{Chl\text{-}a}\ l^{-1}$: Figure 11 dotted lines) when this oscillation period decreases (i.e. from yearly to 2 days), the duration of extreme condition periods (*ad libitum* or starvation) decreases. Thus, an increase in the duration of these extreme conditions results in a decrease in the time required to reach commercial size (29 to 24 months; Figure 11A) and, at the same time, a decrease in reproductive effort (4 to 0 spawning events; Figure 11B.

For the above food scenarios, the total amount of food available on a given period of time is mostly driven by the duration of the oscillations rather than the

amplitude of the oscillations. Consequently, for a given amplitude, the differences between life history traits is driven by recovery after starvation. This had a major impact on reproduction. For instance, for an amplitude cycle of 0.6 $\mu g_{Chl\text{-}a}\ l^{-1}$ no reproduction is allowed for oscillation periods between 1.5 to 3 months (Figure 11 B). Conversely, energy distribution lead oysters to slow growth at high oscillation period and vice versa (Figure 11 A).

No differences were reported on the PLD for amplitude of variations under 0.2 µg Chl-a l^{-1} and/or turnover rates faster than one month with a time of 20 days required to reach settlement (not shown). Otherwise, PLD ranged from 20 to 70 days if the cycle of food variation started with a decrease and ranked from 10 to 20 in case of an increase.

Discussion

Critical examination of the new DEB model calibration

The new DEB calibration for *P. margaritifera* leads to one single model with primary parameters applicable all along the life cycle. Compared to previous DEB models applied to *P. margaritifera* that described separately larvae and adult phases (Fournier, 2011; Thomas et al., 2011), the new full life cycle calibration brings together a wide range of datasets ranging from simple age at birth to respiration curve at different food level and temperature. By considering all life stages in a single model, this new DEB model for *P. margaritifera* is more suitable for future ecotoxicological, physiological or biophysical ecology investigation. This is also a first step towards integrated population and ecosystem dynamic models.

Compared to the larval and adult phase DEB models (Fournier, 2011; Thomas et al., 2011), we obtained different parameter values for the metabolic rates at the reference temperature of 20°C. For instance; the general specific cost of maintenance $[\dot{p}_M]$ that was previously calibrated at 24 and 54 J cm^{-3} d^{-1} for the larvae and adults respectively dropped to a common value of 5.4 J cm^{-3} d^{-1} in this study. This compound parameter is directly related to the allocation fraction to soma (κ) and the maximum surface-specific assimilation rate ($\{p_{Am}\}$), thus the new calibration induces an increase of κ from 0.45 and 0.53 respectively for larvae and adult to 0.75, and a decrease of $\{p_{Am}\}$ from 13 and 795 respectively for larvae and adult to 3.06 J cm^{-2} d^{-1}. The newly calibrated value of κ and $\{p_{Am}\}$ remain consistent with the general patterns identified

for bivalves (Kooijman, 2013) e.g., *Tridacna gigas,* a tropical bivalve had a κ of 0.83 and a $\{p_{Am}\}$ of 5.11 J cm^{-2} d^{-1} at the reference temperature of 20°C.

Moving from two separated models to one single model did not affect thus far the description of the different life stages. Growth curves were well captured with $R^2 >$ 0.9. Previous (Fournier, 2011) and new DEB models respected the general patterns of observed mean flesh mass and reproductive effort. Model construction prioritized maintenance before growth and reproduction, and no maintenance cost could be paid from structure. Therefore in poor conditions, shell growth (that is a proxy for structural growth) stopped while flesh mass or reproduction buffer decreased, which is in agreement with observed patterns (Chávez-Villalba et al., 2013; Linard et al., 2011). In the model, the differences between compartment (reserve, structure and reproduction buffer) dynamics implied that the various life history traits were not reproduced with the same accuracy along the entire life cycle. For instance, shell growths were the best fitted measurements at any life stage and for any type of environments (Figure 4; Figure 8). Conversely, flesh dry masses accuracy was more variable across time, with achieved R^2 depending on the age class ranging from 0.56 to 0.91 (Figure 5; Figure 6 A). This is consistent with the idea that weight fluctuates within individual of the same length and that inter-individual variability increases with age (Pace et al., 2006).

Regarding gameto-somatic index (*GamSI*) evolution, the model was less accurate (Figure 7 C & D), with low R^2 and substantial dissimilarity between observed and simulated patterns. The discrepancies translate some difficulties for the model to accurately capture gametogenesis variations and spawning events in a variable environment. Part of the variance might be due to the sampling mode, which is lethal. Hence, the measured cohorts were different at each time-step, while simulations referred to a single cohort only. Thus, the initial conditions of each sampling point could differ. In addition, the sensitivity to this initial condition was likely more acute, considering the chosen reproduction “opportunistic strategy” (Le Moullac et al., 2012; Pouvreau et al., 2000c). This modelling strategy does not consider endogenous or exogenous factors assumed to favor the synchronicity of spawning (Southgate and Lucas, 2011) and it is thus difficult to reproduce accurately the sudden decrease of *GamSI* as observed in the field. A non-lethal sampling mode such as the high-frequency non-invasive (HFNI) valvometry that can record spawning event from the valves activity (Bernard et al., 2016) might improve model outputs and general understanding of spawning determinism.

Conservative versus lethal sampling and simulation strategies cannot explain alone the general underestimation of flesh dry mass that was modeled in Gambier for

several months, e.g. from February to May (Figure 6 A). A more likely explanation could be a lack of accuracy regarding the description of the amount of energy available in the field by using total chlorophyll-a as proxy for food. This last hypothesis is reinforced by the need to keep the half saturation coefficient (X_k) as a free-fitting parameter. As Alunno-Bruscia et al. (2011) has previously described for *C. gigas,* X_k integrates all variations related to the trophic environment. This includes food sources, variations of food nutritive quality, different selection of the filtered particles and variability in assimilation efficiency according to the particles actually ingested. As such, the presence of a food source that is poorly or not captured by the chlorophyll-a might explain the disagreement between observations and simulations of weight (Picoche et al., 2014). It is known for other bivalves (Sauriau and Kang, 2000) that filtration, selection, and ingestion capacities depend on life stage or on prey sizes. Overall, high values correspond to poor trophic quality or low appetence for the available food. From there, the model suggests that cultivated micro-algae are less appropriate to feed pearl oysters than *in situ* species (Validation dataset 1) and *in situ* phytoplankton is more palatable for growing oysters (Validation dataset 2). These results remain consistent with the fact that *P. margaritifera* also feed *in situ* on achlorophyllous organisms. Following the work of Fournier (2011) and Picoche et al. (2014), further work on pearl oyster trophic regime, planktonic communities and their nutritional value would be warranted, jointly with weight measurement.

Sensitivity analysis to environmental conditions

The constant behavior of temperature and food availability conditions in simulation 1 did not correspond to a real environment. However, as mean annual temperature is function of the latitude and mean chl-a concentration function of the lagoon water residence time (Andréfouët et al., 2001; Delesalle and Sournia, 1992) fixing in such a way the mean annual values created a partition between lagoons with different potentials and modes for oyster production. Lagoons from the northern Tuamotu Archipelago experience higher mean annual temperature than those experienced by the Gambier Islands and first appear to be more suitable for oysters' growth (Figure 9). However due to different food qualities (suggested by different values of X_k and based on the standard mean annual value of 0.2 $\mu g_{Chl\text{-}a}\ l^{-1}$), the performances are better in Gambier than northern Tuamotu. Thus far, PLD data are unavailable for Gambier. This prevents the appropriate adjustment of X_k and the assessment of model predictions. But for growth until commercial sizes are reached,

651 the simulations agreed with Pouvreau and Prasil (2001) observations, with 24 and 25
652 months respectively in the Gambier and northern Tuamotu to reach 10 cm. These
653 results highlight the need to take into account food quality jointly with temperature to
654 explain past pearl farming performances, and in anticipation of environmental changes
655 for planning future farming.

656 High seasonal temperature fluctuation had for general impact to decrease
657 growth and reproductive effort, modulo the mean annual value (Figure 10). From
658 simulation 2, performances decreased jointly with rising seasonal variations but this
659 sensitivity to seasonal fluctuation declined when the mean temperature dropped. In
660 French Polynesia, small seasonal variations are associated with high mean annual
661 temperatures and vice versa. According to energetic dynamics, increasing
662 temperatures accelerate energetic flux until an optimum, thus high temperature
663 variations introduce a seasonality in reproduction with increased spawning during the
664 warm season. The role of seasonal temperature variations and phytoplankton blooms
665 on bivalve reproduction and synchronicity has been demonstrated for species in
666 temperate environments (e.g. Philippart et al., 2012; Ruiz et al., 1992). To assess the
667 influence of the environment on the *P. margaritifera* reproduction "opportunistic
668 strategy" described by Fournier et al., (2012), it could be useful to sample *GamSI* along
669 a gradient of atolls that experiment various temperature seasonal differences. This
670 way, it would be also easier to further assess the influence of various endogenous or
671 exogenous factors in spawning synchronicity.
672
673 Simulation 3 suggested contrasted responses of the black-lipped pearl oyster
674 to phytoplankton biomass fluctuations. Energetic dynamics implies that oysters
675 accessing similar amount of food (cumulative) but with different variations of
676 concentrations across time will react differently. In particular, the duration of extreme
677 condition periods implies different recovery needs after starvation and the
678 consequences are expressed in the life history traits. For instance, gametogenesis
679 duration has to be taken into consideration to explain the patchy results in simulation
680 3. Above the reference food concentration, the proximity between gametogenesis
681 completion time and oscillation period prevented the reproduction buffer from filling up
682 completely during the plenty period. The oyster became unable to reproduce, while in
683 the same time the cumulative amount of food available in the environment is supposed
684 to allow 5 spawns within a year (Figure 9 B). In agreement with Fournier et al. (2012)
685 and Pouvreau et al. (2000c) who linked food concentration with reproductive effort and

synchronicity, simulation 3 confirms that food availability is the main driver of reproduction.

The results from the three theoretical scenarios highlight the importance of environmental variations rather than mean annual conditions to model and infer physiological traits. Food and temperature variations have significant impact on energy dynamics since temperature drives the speed of exchanges between compartments and food controls the amount of energy in circulation. Simulating a constant environment cannot reproduce the low physiological performances induced by environmental fluctuations, such as the compensation during starvation periods by reserves or the differences of energetic flux kinetics following temperature variation. Practically, the absence of a regular, predictable, time interval between plenty and starvation periods, makes difficult to infer the best possible locations for pearl farming.

The range of conditions represented by the various simulations had no impact on larval development. This is due to the time scale which are significantly different between pelagic larval duration and environmental changes in our simulations. At small time scale, PLD ranging from 10 to 70 days (the maximal theoretical values from our simulations) are simulated depending on the season and/or the trajectory (up or down) taken by the food availability variation (simulations 1 & 3). The 70-day extreme PLD has never been observed and will probably seldom occur in realistic environment with all mortality causes present (disease, predation…). Significant variations of temperature and food concentration are reported at short space and time intervals within a given lagoon (Thomas et al., 2010). Thus, mortality rate, environmental heterogeneity and larval behavior partly explain the 15 to 35 days PLD reported in the literature (Sangare et al., 2019; Thomas et al., 2014). Here, the results indirectly confirm that a spatial environmental heterogeneity plays a significant role in recruitment, by influencing growth rate, and indirectly mortality and dispersion time. High frequency monitoring of the environment in space and time emerge as a critical bottleneck for realistic modeling of larvae development and dispersal.

Perspectives

According to this study, most of the existing data on *in situ* growth and reproduction for *P. margaritifera* agree with the results of the DEB model when considering adequate food and temperature variations. Thus, adequately considering

720 future environmental conditions may provide insights in the future trends of *P.*
721 *margaritifera* life history traits expression. In the next few decades, changes in ocean
722 currents and temperature are projected to alter the surface and productivity of
723 ecological areas near the South Pacific subtropical gyre leading to reduced
724 phytoplankton biomass and average size in the ocean, which may also impact lagoons
725 (Bell et al., 2013). Adult *P. margaritifera* feed preferentially on planktonic organism
726 larger than 2 µm (Fournier et al., 2012a; Loret et al., 2000) and according to our model
727 simulations, such changes could affect pearl oyster reproduction and growth, and
728 eventually pearl farming yields. It would be interesting in the future to monitor the
729 environmental changes and track the trajectories followed by each lagoon ecosystem
730 within our simulation space, and infer possible problems. Obviously, simulations
731 remain coarse simplification of the real environment, and various other factors might
732 temperate the results. This could include fast environmental variations as well as
733 physiological or genetical adaptations. Few studies have looked at the role of genetics
734 in shaping pearl oyster life traits and thus on the potential of adaptation to changing
735 conditions. Joubert et al. (2014) investigated the environmental control underlying the
736 molecular mechanisms of shell growth, and Ky and Le Moullac (2017) highlighted the
737 non negligible part of genetics on growth variability. We suggest that further work on
738 these aspects is warranted.
739 At the intra-lagoon scale, phytoplankton abundance is highly dependent on
740 water exchange from the ocean through the atoll rim but the influence of pearl farming
741 activity itself on plankton concentration should not be overlooked. Lefebvre et al.
742 (2012), Pagano et al. (2017) and Hulot et al. (2018) suggested significant depletion of
743 planktonic organism concentration in aquaculture areas, which can be induced by tidal
744 flushing and by the grazing pressure of the filter-feeder communities. Long periods of
745 low phytoplankton biomass followed by intense sporadic blooms have been reported
746 in French Polynesian atolls lagoons (Sakka et al., 1999) but, lack of high frequency
747 data on phytoplankton communities and biomass makes difficult to accurately
748 characterize the magnitudes and periods of these events, and the role of pearl farming
749 itself on these mechanisms.
750 Finally, to scale-up the limit of the black-lipped pearl oyster response to the
751 environment conditions, a suggested approach would be i) the integration of the DEB
752 model into an individual-based model for the population level (Bacher and Gangnery,
753 2006; Thomas et al., 2016b, Sangare et al. in prep.) ii) coupling this population model
754 with a biogeochemical and an environmental model able to provide food, temperature
755 and the conditions of larval transport. Such design would expand the work of Thomas
756 et al. (2016a) on *P. margaritifera* who characterized larval growth and dispersal in a

dynamic environment by coupling the DEB model for larvae with a hydrodynamic model.

Conclusion

By its ability to accurately describe a wide range of *P. margaritifera* physiological traits in contrasted environment, the calibrated full life cycle DEB model provides new opportunities to address questions spanning from physiological limits and adaptations to pearl farming sustainability. From the tested environmental scenarios, the simulations shed light on the influence of variations of temperature, food availability and quality on *P. margaritifera* life history traits expression. From both the environmental and physiological point of view, more observations are required for a better assessment of reproduction potential. Adequately considering future environmental conditions and testing them within this new calibrated DEB model may provide a powerful tool contributing to the sustainable management of marine resources and their associated ecological issues.

Acknowledgements

This study was co-funded by the Institut français de recherche pour l'exploitation de la mer (IFREMER) and the Direction des Ressources Marines et Minières de Polynésie française (DRMM). Support was also provided through the ANR-16-CE32-0004 MANA (Management of Atolls) project. The authors thank the IFREMER and DRMM teams who participated in the experiments conducted at Vairao. A special thanks to Caline Basset for her invaluable help during the acquisition and the processing of the field data as well as Augustin Mata and Judy Mata for having welcomed us on the beautiful atoll of Ahe and allowed to work in the best conditions.

783 Table 1 Datasets used for model validation.

Dataset		Site	Observation	Life stage	Survey period	Environment	Reference
1	A	Ahe	Shell length	Larvae	End of Austral summer (April-May)	Larval rearing of 20 days in an open circuit with a diet of cultured algae *Isochrisis affinis galbana* and *Chaetoceros sp. jonquieri* in a 1:1 cell ratio	(Thomas et al., 2011)
	B					Larval rearing of 15 days conducted in the Ahe lagoon, with an open circuit rearing system supplied with lagoon water pre-filtered at 40 µm	
	C					Larval rearing of 15 days conducted in the lagoon, performed in microcosm (net mesh 40 µm, volume 250 l) in the water of the Ahe lagoon	
	D					Cohort of 'wild' larvae collected in water samples taken every two days in the Ahe lagoon	
2		Takapoto	Flesh dry weights	Adults (3 cohorts of 1; 2 & 3 years old)	Full year	*In-situ* rearing	(Pouvreau et al., 2000a)
3		Gambier	Flesh dry weights	Adults	Full year	*In-situ* rearing	(Le Moullac et al., 2012)
4	A	Ahe	Reproductive effort	Adults	6 months from mid-austral summer to mid-austral winter (February -August)	*In-situ* rearing at 2 environmentally contrasted sampling stations (Fig. 1)	(This study)
	B		Shell length	Adults (2 cohorts of 1.5 & 3.5 years old)			

784

785

Table 2 Symbols and parameters values at the reference temperature T_{ref} = 293.15 °K. Values annotated by a letter have been calibrated directly using literature data, other values were calibrated according to the *AmP* procedure (Marques et al., 2018).

Symbol	Value	Units	Description
		Primary DEB parameters	
$\{\dot{p}_{Am}\}$	0.055 - 3.065	J cm^{-2} d^{-1}	Maximum surface-specific assimilation rate before (left) and after (right) acceleration
κ_X	0.416	-	Digestion efficiency of food to reserve
$[E_G]$	2383.2	J cm^{-3}	Volume-spec. cost for structure
$\dot{v}$	0.0002 - 0.01	cm d^{-1}	Energy conductance before (left) and after (right) acceleration
$[\dot{p}_M]$	5.39	J d^{-1} cm^{-3}	Volume-spec. somatic maintenance
$\dot{k}_J$	1.638×10^{-3}	d^{-1}	Maturity maintenance rate coefficient
κ	0.75	-	Allocation fraction to soma
κ_R	0.25	-	Reproduction efficiency
E_0	2.764×10^{-4} [b]	J	Egg energy content
E_{Hb}	6.326×10^{-5}	J	Maturity at settlement
E_{Hs}	3.537×10^{-4}	J	Maturity at settlement
E_{Hj}	3.011	J	Maturity at metamorphosis
E_{Hp}	3015	J	Maturity at puberty
		Auxiliary parameters	
T_A	5785	K	Arrhenius temperature
T_L	291.77 [a]	K	Lower temperature boundary
T_H	306.83 [a]	K	Upper temperature boundary
T_{AL}	137.61	K	Arrhenius temperature for lower boundary
T_{AH}	303407	K	Arrhenius temperature for upper boundary
δ_M	0.27	-	Shape coefficient
$\delta_{M\ larv}$	0.59	-	Shape coefficient before metamorphosis
d_V	0.09	g.cm^{-3}	Specific dry density of structure
w_E	23.9	g.mol^{-1}	Specific dry weight of reserve
μ_E	550 000	J.mol^{-1}	Chemical potential of reserve
X_K	0.2 [f]	$\mu g_{Chl\text{-}a}$ l^{-1}	Half-saturation coefficient for adults fed *ad libitum* in laboratory
$X_{K\ larv}$	0.6 [e]	$\mu g_{Chl\text{-}a}$ l^{-1}	Half-saturation coefficient for larvae fed *ad libitum* in laboratory
$GamSI_{Threshold}$	0.29 [c]	-	Gonado-somatic index triggering spawning
SpawnRatio	0.85 [d; f]	-	Proportion of the reproduction buffer emptied at each spawning

[a] (Le Moullac et al., 2016); [b] (Acosta-Salmón, 2004); [c] (Pouvreau et al., 2000a); [d] (Fournier, 2011); [e] (Sangare et al., 2019); [f] personal unpublished data

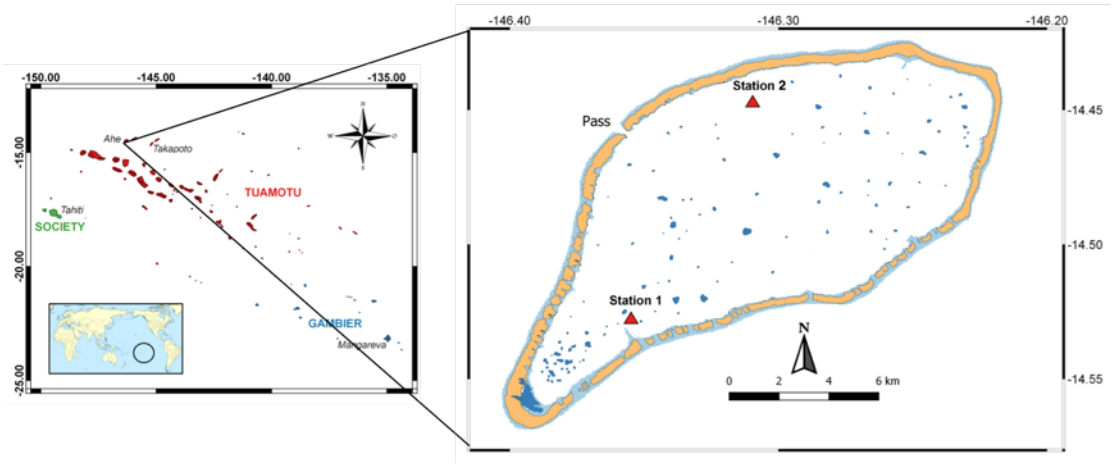

792

793

794 Figure 1 Location of Ahe atoll and location of experimental sampling stations in the

795 lagoon.

796

797

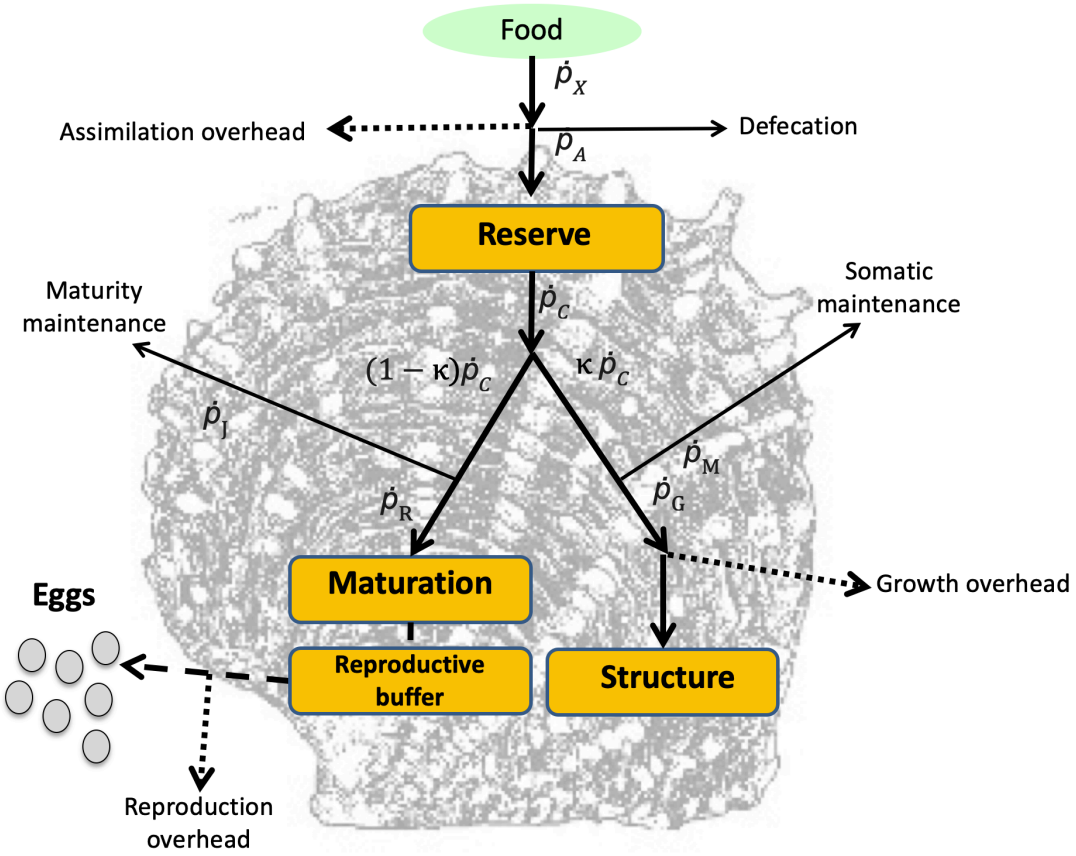

798

799 Figure 2 Schematic representation of a dynamic energy budget of black-lipped pearl
800 oyster. Energy fluxes (solid arrows) and state variables (orange boxes) are defined in
801 Appendix A. Overheads are represented by dotted arrows.

802

803

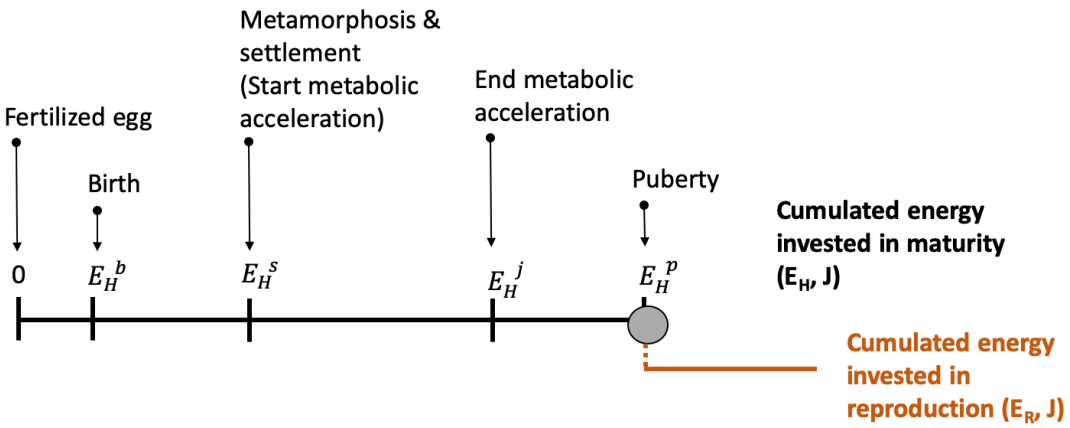

804

805 Figure 3 Definition of the different life stages in the DEB model. Between conception
806 ($E_H = 0$) and birth ($E_H = E_H^b$) there is no external assimilation. Assimilation is switched
807 on after birth. After birth at maturity level $E_H = E_H^s$ the organism metamorphosis and
808 starts metabolic acceleration which ends at juvenile stage ($E_H = E_H^j$). After puberty (E_H
809 $= E_H^p$), i.e. the adult stage, allocation towards maturation stops and allocation towards
810 reproduction starts (modified from Augustine et al., 2014).

811

812

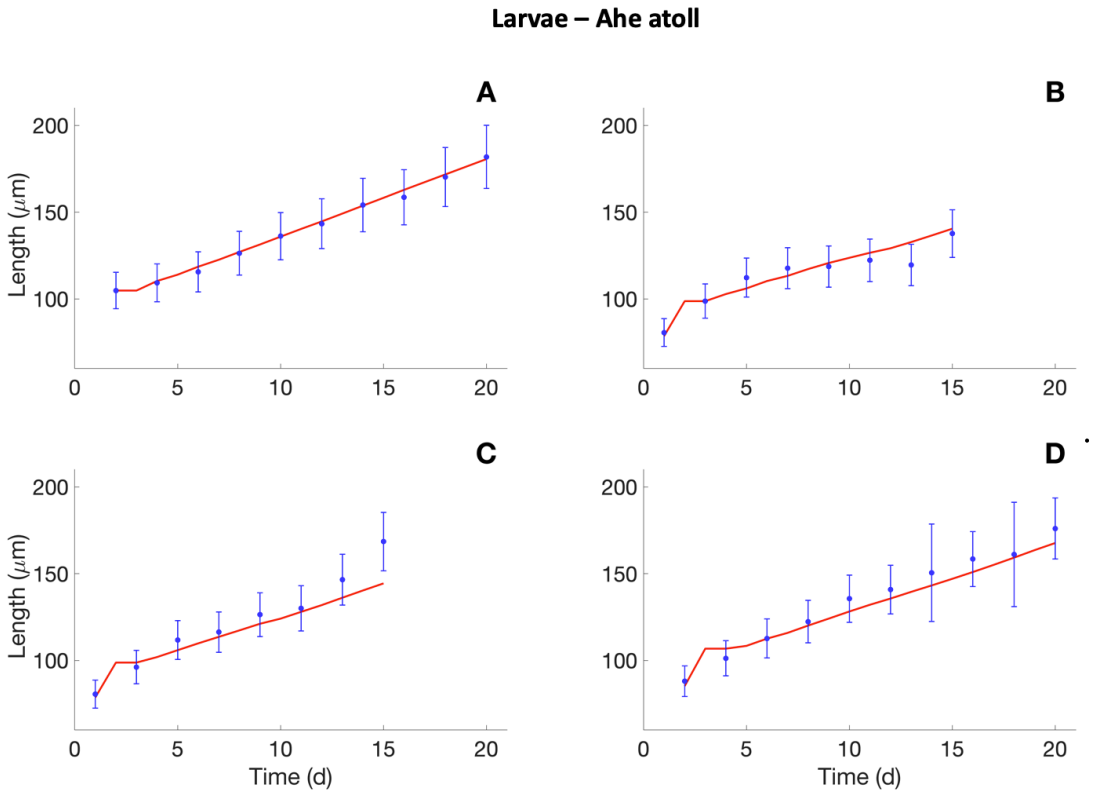

813

814 Figure 4 Comparison of observed (points ± standard deviation) and simulated (line)
815 larval shell growth of *P. margaritifera*: (A) rearing in an open circuit with cultured
816 algae as a food supply (X_k= 0.60 $\mu g_{Chl\text{-}a}\ l^{-1}$), (B) rearing in an open circuit with water
817 from the Ahe lagoon (X_k= 0.20 $\mu g_{Chl\text{-}a}\ l^{-1}$), (C) rearing in a microcosm in the Ahe lagoon
818 (X_k= 0.20 $\mu g_{Chl\text{-}a}\ l^{-1}$), (D) cohort identified *in situ*, in the Ahe lagoon (X_k= 0.20 $\mu g_{Chl\text{-}a}$
819 l^{-1}).

820

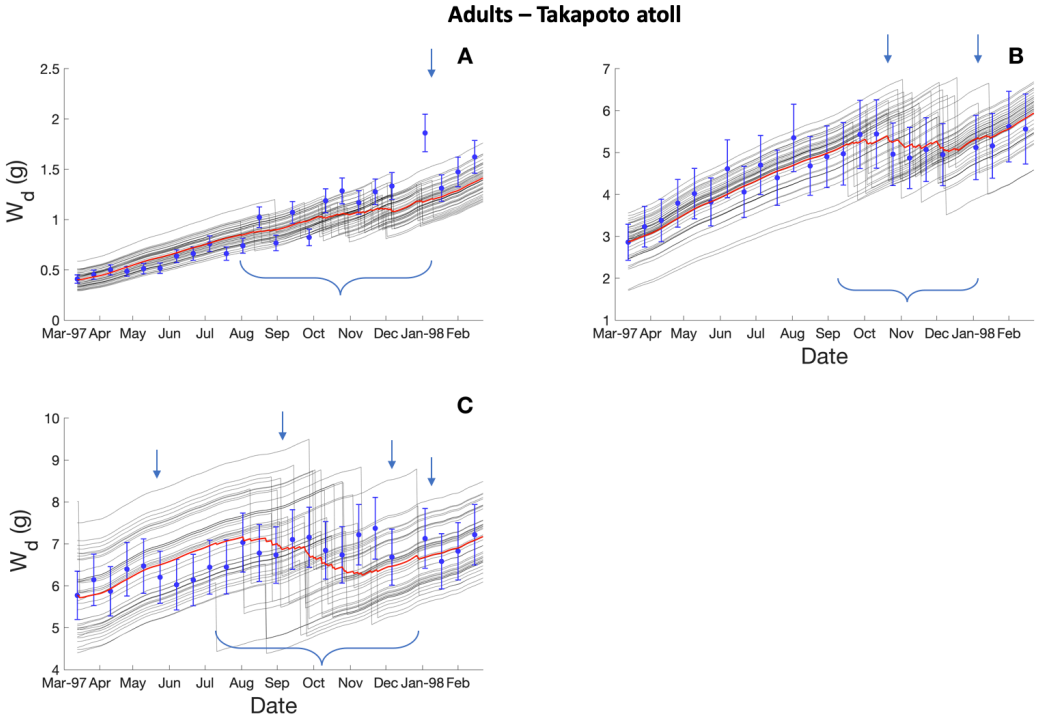

Figure 5 Growth in dry weight for age group 1 (A), 2 (B) and 3 (C) of pearl oysters (observed mean ± standard deviation = symbols; individual simulations = thin lines) in Takapoto atoll lagoon during 365 days. The bold lines represent the mean value of the individual simulations (n = 30), the braces refers to the simulation based spawning periods and arrows refer to spawning events identified by Pouvreau et al., 2000a.

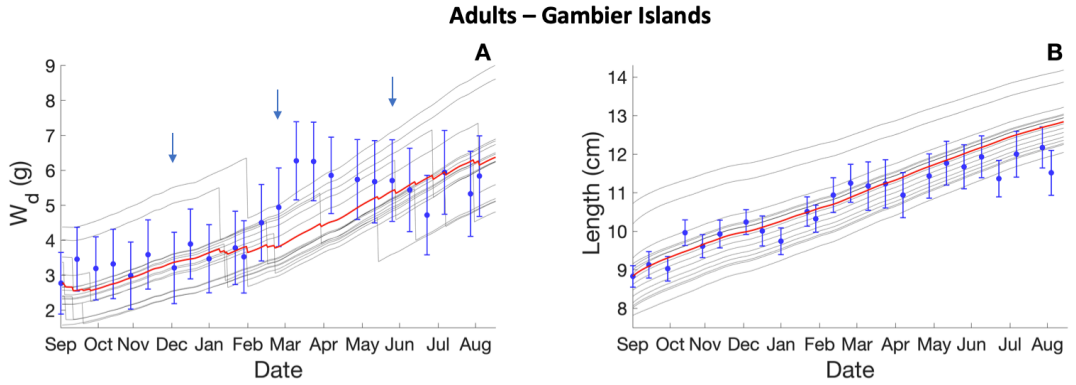

Figure 6 Evolution of flesh dry mass (A) and shell length (B) in Gambier Islands. Points and bars represent the observed mean ± standard deviation; thin lines refer to individual simulations and the bold lines represent the mean value of the individual simulations. Arrows refer to spawning events recorded by Le Moullac et al., 2012.

836

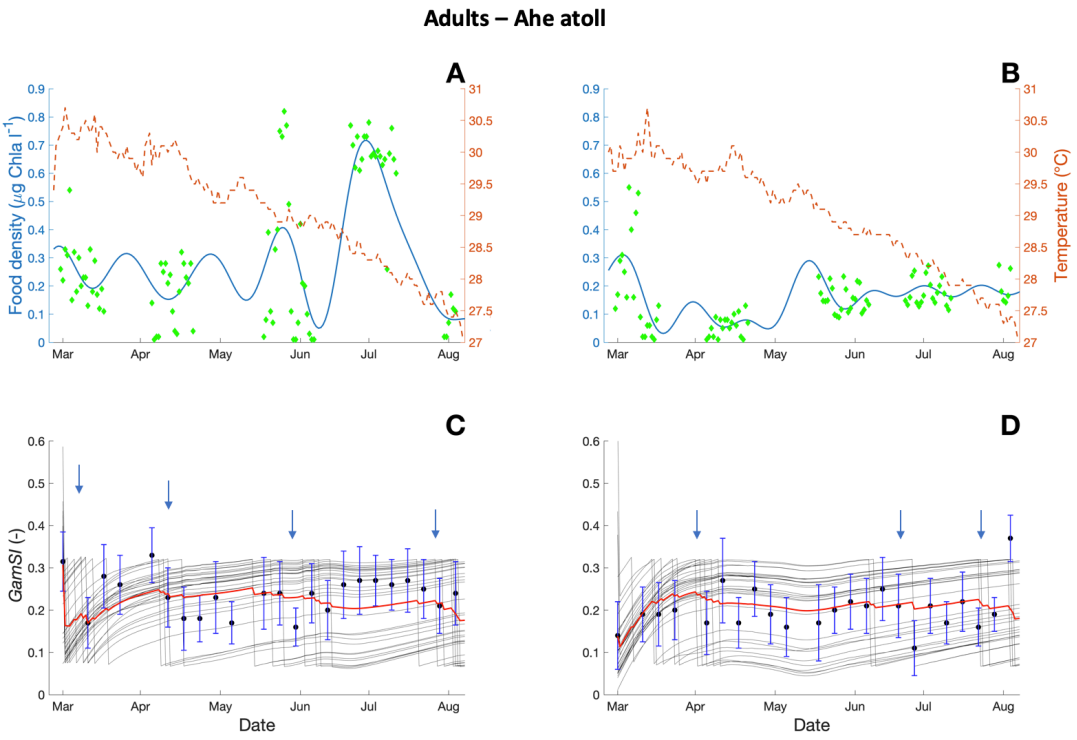

837

838 **Figure 7 Variation of temperature (dashed line) and chlorophyll-a concentration from Fourier series (solid**
839 **line) computed from in situ measurements (points) at the station 1 (A) and 3 (B). Comparison of observed**
840 **mean *GamSI* ± standard deviation (points) and individual simulations (thin lines) at the sampling stations 1**
841 **(C) and 3 (D); bold solid lines represent the mean value of the individual simulations. Individual spawning**
842 **events correspond to drops in the thin lines and arrows refer to potential spawning events.**

843

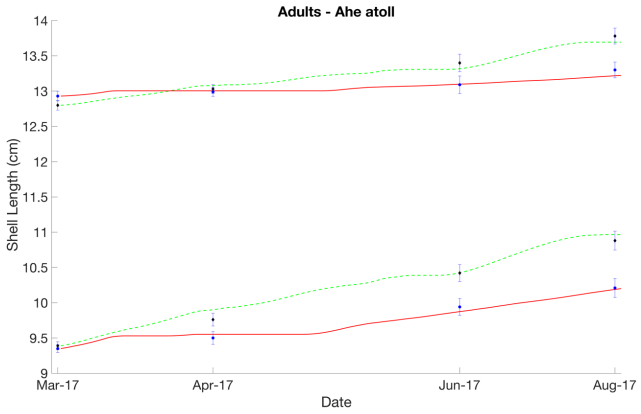

Figure 8 Shell length evolution of the mean observed values at sampling station 1 (diamonds) and 3 (circles) and simulations at sampling station 1 (solid lines) and 3 (dotted lines) for two classes of sizes in the lagoon of Ahe in 2017.

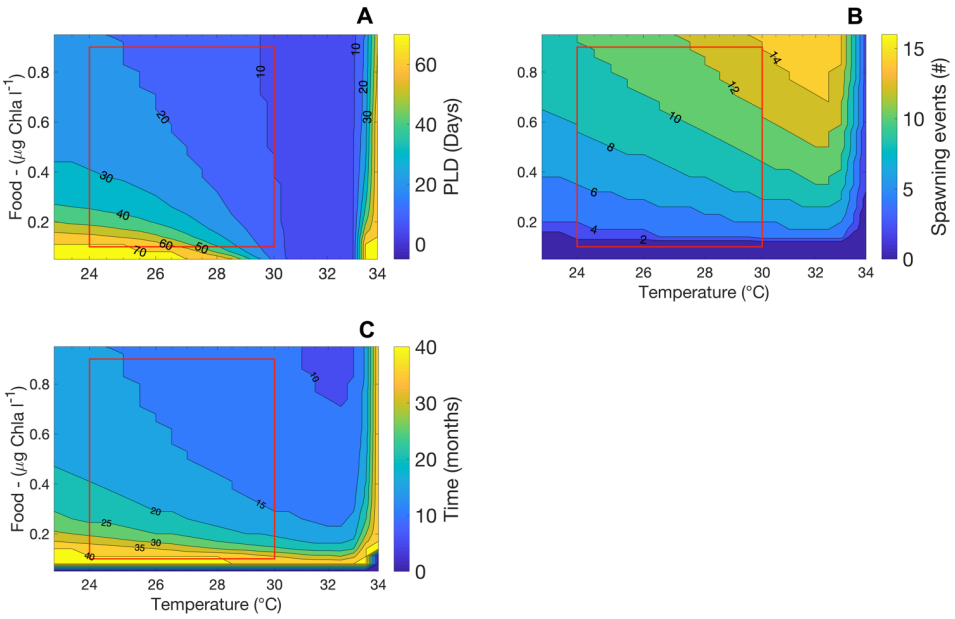

Figure 9 Theoretical simulations illustrating the influence of temperature an food concentration (assumed to be constant over time) on life-history traits: (A) pelagic larval duration (Xk = 0.6 $\mu g_{Chl\text{-}a}\ l^{-1}$), (B) yearly reproductive effort (number of spawning events) for a 13 cm shell length individual (Xk = 0.2 $\mu g_{Chl\text{-}a}\ l^{-1}$) and (C) time required to reach commercial size for a young collected spat (Xk = 0.2 $\mu g_{Chl\text{-}a}\ l^{-1}$). Rectangles encapsulate the environmental conditions observed in French Polynesian atoll lagoons.

858

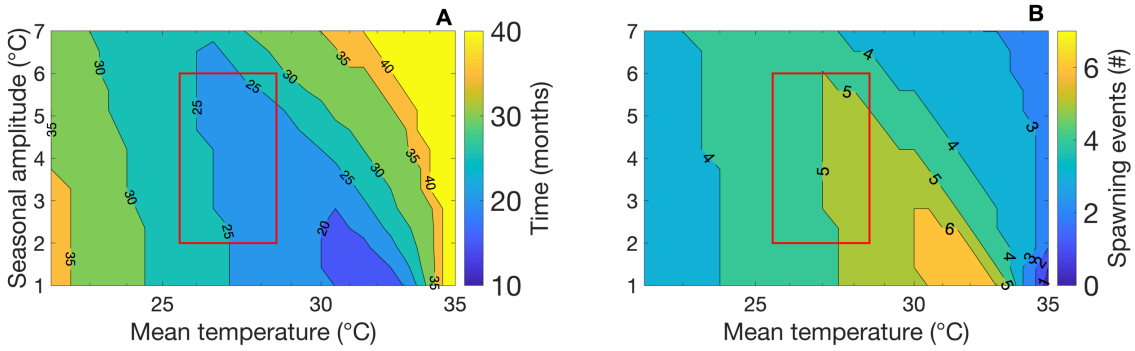

859

860 **Figure 10 Influence of yearly temperature amplitude and yearly mean temperature on (A) the time required**
861 **to reach commercial size for a young collected spat (B) reproductive effort (number of spawns) of a 13 cm**
862 **shell length individual within a year. Simulation with constant food of 0.2 $\mu g_{Chl\text{-}a}\ l^{-1}$ and Xk = $\mu g_{Chl\text{-}a}\ l^{-1}$.**
863 **Rectangles encapsulate the environmental conditions observed in French Polynesian atoll lagoons.**

864

865

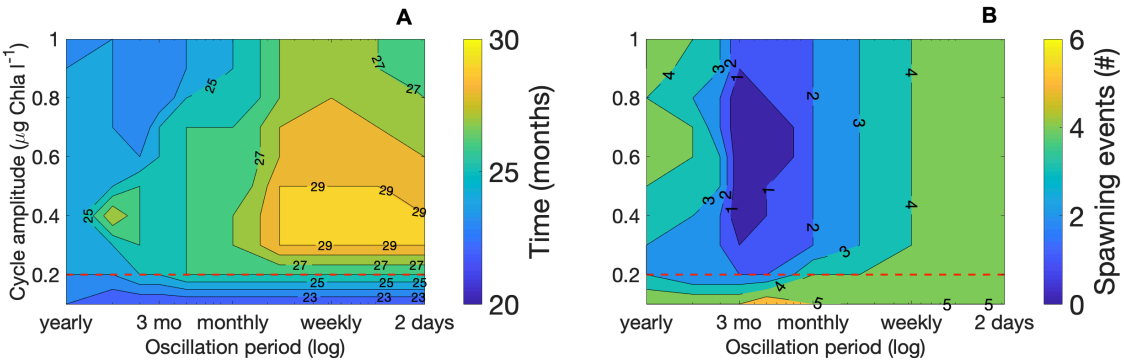

866

867 **Figure 11 Influence of stability of phytoplankton biomass represented by the chl-a cycle amplitude (y-axis)**
868 **and the oscillation period of chl-a cycles (x-axis) on (A) time required to reach commercial size for a young**
869 **collected spat and (B) reproductive effort (number of spawns) of a 13 cm shell length individual within a year.**
870 **Dotted lines refer to the reference value around which food variations (i.e. cycle amplitudes from 0.1 to 1**
871 **$\mu g_{Chl\text{-}a}\ l^{-1}$) oscillate.**

872

Appendix A

Equations of the metabolic fluxes

DEB theory pictures an organism into mass and energy symbolized by four state variables: reserves (E, J), structural volume (V, cm^3), maturity (E_H, J) and reproduction buffer (E_R, J). The conceptual scheme of the model is described in Figure 2. Energy enters the organism as food (X) thanks to a Holling type II functional response and is assimilated at a rate of ($\dot{p}_A$, J day^{-1}) into reserves. The mobilization rate ($\dot{p}_C$, J day^{-1}) controls the energy outflow from the reserve to cover somatic ($\dot{p}_M$, J day^{-1}) and maturity ($\dot{p}_J$, J day^{-1}) maintenance, structural growth ($\dot{p}_G$, J day^{-1}) and maturation then reproduction ($\dot{p}_R$, J day^{-1}) before and after puberty respectively. Assimilation is a function of food availability, following functional response when mobilization is determined by the energy stored into the reserve compartment. κ is the proportion of the energy mobilized from the reserve compartment to the structural maintenance and growth $\dot{p}_M$ and $\dot{p}_G$, while the rest (1 - κ) is used for maturity maintenance and reproduction buffer filling, $\dot{p}_J$ and $\dot{p}_R$. Physiological rates, such as ingestion and maintenance, depend on environmental temperature. This relation is described by an Arrhenius-type equation within a species-specific tolerance range between upper and lower temperature boundaries (Kooijman, 2010).

Table S1 Dynamic energy budget model equations

Fluxes (J d^{-1})	
Feeding rate	$\dot{p}_X = \{\dot{p}_{Xm}\} \cdot \boldsymbol{f} \cdot V^{2/3}$
Assimilation rate	$\dot{p}_A = \dot{p}_X \cdot \boldsymbol{\kappa_x} \cdot s_M$
Utilization rate	$\dot{p}_C = E \cdot \left(\frac{[E_G] \cdot \dot{v} \cdot V^{2/3} \cdot s_M + \dot{p}_M}{\kappa \cdot E + [E_G] \cdot V} \right)$
Somatic maintenance rate	$\dot{p}_M = [\dot{p}_M] \cdot \boldsymbol{V}$
Maturity maintenance rate	$\dot{p}_J = k_J \cdot E_H$
Growth rate	$\dot{p}_G = \kappa \cdot \dot{p}_C - \dot{p}_M$
Reproduction / maturity rate	$\dot{p}_R = (1 - \kappa) \cdot \dot{p}_C - \dot{p}_j$
Correction factors	

Acceleration factor with: $L = V^{1/3}$; L_s: length at settlement and L_j length at juvenile stage	$$s_M = \begin{cases} 1 , & E_H < E_{Hs} \\ L/L_s , & E_{Hs} \le E_H < E_{Hj} \\ L_j/L_s , & E_{Hj} \le E_H \end{cases}$$
Temperature correction factor	$$C_T = exp\left\{\frac{T_A}{T_{ref}} - \frac{T_A}{T}\right\} \cdot \left(1 + exp\left\{\frac{T_{AL}}{T_{ref}} - \frac{T_{AL}}{T_L}\right\} + exp\left\{\frac{T_{AH}}{T_H} - \frac{T_{AH}}{T_{ref}}\right\}\right) \cdot \left(1 + exp\left\{\frac{T_{AL}}{T} - \frac{T_{AL}}{T_L}\right\} + exp\left\{\frac{T_{AH}}{T_H} - \frac{T_{AH}}{T}\right\}\right)^{-1}$$
Differential equations	
Reserve dynamic	$$\frac{d}{dt}E = \dot{p}_A - \dot{p}_C$$
Structural body volume dynamic	$$\frac{d}{dt}V = \frac{\dot{p}_G}{[E_G]}$$
Dynamics for energy allocated to maturation, when $E_H < E_H^p$	$$\frac{d}{dt}E_H = (1-\kappa)\cdot \dot{p}_C - \dot{p}_J$$ With $\frac{d}{dt}E_R = 0$
Dynamics for energy allocated to reproduction, when $E_H \ge E_H^p$	$$\frac{d}{dt}E_R = (1-\kappa)\cdot \dot{p}_C - \dot{p}_J$$ With $\frac{d}{dt}E_H = 0$

Appendix B

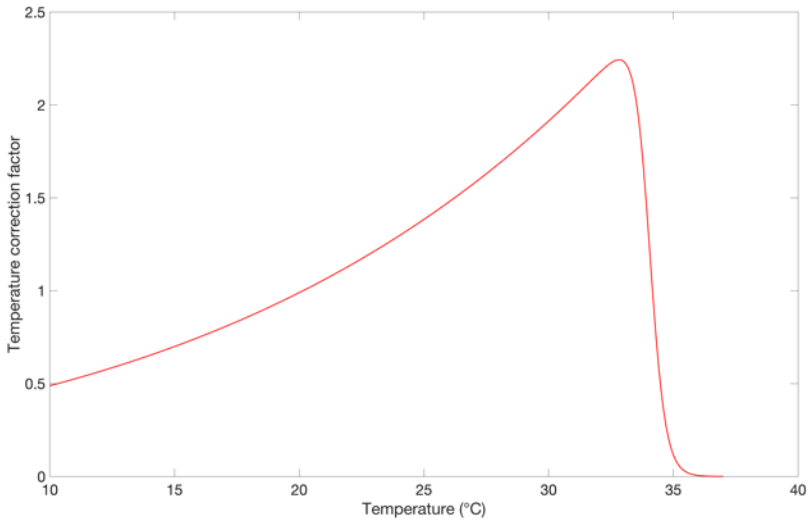

Figure S1 Effect of temperature on physiological rates. The temperature correction factor (see Appendix A Table S1 for formulation and Table 2 for parameter values) is applied on energy fluxes according to the body temperature.

References

Acosta-Salmón, H., 2004. Broodstock management and egg quality of the pearl oysters Pinctada margaritifera and Pinctada fucata.

Alunno-Bruscia, M., Bourlès, Y., Maurer, D., Robert, S., Mazurié, J., Gangnery, A., Goulletquer, P., Pouvreau, S., 2011. A single bio-energetics growth and reproduction model for the oyster Crassostrea gigas in six Atlantic ecosystems. J. Sea Res. 66, 340–348. https://doi.org/10.1016/J.SEARES.2011.07.008

Andréfouët, S., Charpy, L., Lo-Yat, A., Lo, C., 2012. Recent research for pearl oyster aquaculture management in French Polynesia.

Andréfouët, S., Pagès, J., Tartinville, B., 2001. Water renewal time for classification of atoll lagoons in the Tuamotu Archipelago (French Polynesia). Coral Reefs 20, 399–408. https://doi.org/10.1007/s00338-001-0190-9

Andréfouët, S., Van Wynsberge, S., Kabbadj, L., Wabnitz, C.C.C., Menkes, C., Tamata, T., Pahuatini, M., Tetairekie, I., Teaka, I., Scha, T.A., Teaka, T., Remoissenet, G., 2018. Adaptive management for the sustainable exploitation of lagoon resources in remote islands: lessons from a massive El Niño-induced giant clam bleaching event in the Tuamotu atolls (French Polynesia). Environ. Conserv. 45, 30–40. https://doi.org/10.1017/s0376892917000212

Augustine, S., Jaspers, C., Kooijman, S.A.L.M., Carlotti, F., Poggiale, J.-C., Freitas, V., van der Veer, H., van Walraven, L., 2014. Mechanisms behind the metabolic flexibility of an invasive comb jelly. J. Sea Res. 94, 156–165. https://doi.org/10.1016/j.seares.2014.09.005

Bacher, C., Gangnery, A., 2006. Use of dynamic energy budget and individual based models to simulate the dynamics of cultivated oyster populations. J. Sea Res. 56, 140–155. https://doi.org/10.1016/J.SEARES.2006.03.004

Bell, J.D., Ganachaud, A., Gehrke, P.C., Griffiths, S.P., Hobday, A.J., Hoegh-Guldberg, O., Johnson, J.E., Le Borgne, R., Lehodey, P., Lough, J.M., 2013. Mixed responses of tropical Pacific fisheries and aquaculture to climate change. Nat. Clim. Chang. 3, 591.

Bernard, I., Massabuau, J.C., Ciret, P., Sow, M., Sottolichio, A., Pouvreau, S., Tran, D., 2016. In situ spawning in a marine broadcast spawner, the Pacific oyster Crassostrea gigas: Timing and environmental triggers. Limnol. Oceanogr. 61, 635–647. https://doi.org/10.1002/lno.10240

Bourlès, Y., Alunno-Bruscia, M., Pouvreau, S., Tollu, G., Leguay, D., Arnaud, C., Goulletquer, P., Kooijman, S.A.L.M., 2009. Modelling growth and reproduction of the Pacific oyster Crassostrea gigas: Advances in the oyster-DEB model

939 through application to a coastal pond. J. Sea Res. 62, 62–71.
940 https://doi.org/10.1016/J.SEARES.2009.03.002
941 Charpy, L., Dufour, P., Garcia, N., 1997. Particulate organic matter in sixteen
942 Tuamotu atoll lagoons (French Polynesia). Mar. Ecol. Prog. Ser. 55–65.
943 Chávez-Villalba, J., Soyez, C., Aurentz, H., Le Moullac, G., 2013. Physiological
944 responses of female and male black-lip pearl oysters (Pinctada margaritifera) to
945 different temperatures and concentrations of food. Aquat. Living Resour. 26,
946 263–271.
947 Delesalle, B., Sakka, A., Legendre, L., Pagès, J., Charpy, L., Loret, P., 2001. The
948 phytoplankton of Takapoto Atoll (Tuamotu Archipelago, French Polynesia): time
949 and space variability of biomass, primary production and composition over 24
950 years. Aquat. Living Resour. 14, 175–182. https://doi.org/10.1016/S0990-
951 7440(00)01098-6
952 Delesalle, B., Sournia, A., 1992. Residence time of water and phytoplankton biomass
953 in coral reef lagoons. Cont. Shelf Res. 12, 939–949.
954 https://doi.org/10.1016/0278-4343(92)90053-M
955 Desforges, J.-P.W., Sonne, C., Dietz, R., 2017. Using energy budgets to combine
956 ecology and toxicology in a mammalian sentinel species. Sci. Rep. 7, 46267.
957 https://doi.org/10.1038/srep46267
958 Doroudi, M., Southgate, P., Mayer, R., 1999. The combined effects of temperature
959 and salinity on embryos and larvae of the black-lip pearl oyster, Pinctada
960 margaritifera (L.). Aquac. Res. 30, 271–277. https://doi.org/10.1046/j.1365-
961 2109.1999.00324.x
962 Dufour, P., Charpy, L., Bonnet, S., Garcia, N., 1999. Phytoplankton nutrient control in
963 the oligotrophic South Pacific subtropical gyre (Tuamotu Archipelago). Mar.
964 Ecol. Prog. Ser. 179, 285–290. https://doi.org/10.3354/meps179285
965 Dumas, F., Le Gendre, R., Thomas, Y., Andréfouët, S., 2012. Tidal flushing and wind
966 driven circulation of Ahe atoll lagoon (Tuamotu Archipelago, French Polynesia)
967 from in situ observations and numerical modelling. Mar. Pollut. Bull. 65, 425–
968 440. https://doi.org/10.1016/J.MARPOLBUL.2012.05.041
969 Fournier, J., 2011. Alimentation et déterminisme environnemental de la reproduction
970 des huîtres perlières P. margaritifera sur l'atoll d'Ahe (Archipel des Tuamotu,
971 Polynésie française), Diet and environmental déterminism of reproduction of
972 pearl oysters P. margaritifera on A.
973 Fournier, J., Dupuy, C., Bouvy, M., Couraudon-Réale, M., Charpy, L., Pouvreau, S.,
974 Le Moullac, G., Le Pennec, M., Cochard, J.-C., 2012a. Pearl oysters Pinctada
975 margaritifera grazing on natural plankton in Ahe atoll lagoon (Tuamotu

976 archipelago, French Polynesia). Mar. Pollut. Bull. 65, 490–499.
977 Fournier, J., Levesque, E., Pouvreau, S., Le Pennec, M., Le Moullac, G., 2012b.
978 Influence of plankton concentration on gametogenesis and spawning of the
979 black lip pearl oyster Pinctada margaritifera in Ahe atoll lagoon (Tuamotu
980 archipelago, French polynesia). Mar. Pollut. Bull.
981 https://doi.org/10.1016/j.marpolbul.2012.03.027
982 Grand, Hauti, 1993. L'aquaculture nacrière et perlière : planches 89-90.
983 Hulot, V., Saulnier, D., Lafabrie, C., Gaertner-Mazouni, N., 2018. Shellfish culture: a
984 complex driver of planktonic communities. Rev. Aquac.
985 https://doi.org/10.1111/raq.12303
986 Hynd, J.S., 1955. A Revision of the Australian Pearl-shells, Genus Pinctada (Lamelli-
987 branchia). Mar. Freshw. Res. 6, 98–138.
988 ISPF, 2016. Le bilan de la perles en 2016. [WWW Document]. URL
989 http://www.ispf.pf/docs/default-source/publi-pf-bilans-et-etudes/pf-bilan-perle-
990 2016.pdf?sfvrsn=6
991 Joubert, C., Linard, C., Le Moullac, G., Soyez, C., Saulnier, D., Teaniniuraitemoana,
992 V., Ky, C.L., Gueguen, Y., 2014. Temperature and Food Influence Shell Growth
993 and Mantle Gene Expression of Shell Matrix Proteins in the Pearl Oyster
994 Pinctada margaritifera. PLoS One 9, e103944.
995 https://doi.org/10.1371/journal.pone.0103944
996 Kooijman, S., 2010. Dynamic energy budget theory for metabolic organisation.
997 Cambridge university press.
998 Kooijman, S.A.L.M., 2014. Metabolic acceleration in animal ontogeny: An
999 evolutionary perspective. J. Sea Res. 94, 128–137.
1000 https://doi.org/10.1016/J.SEARES.2014.06.005
1001 Kooijman, S.A.L.M., 2013. Waste to hurry: dynamic energy budgets explain the need
1002 of wasting to fully exploit blooming resources. Oikos 122, 348–357.
1003 https://doi.org/10.1111/j.1600-0706.2012.00098.x
1004 Kooijman, S.A.L.M., Pecquerie, L., Augustine, S., Jusup, M., 2011. Scenarios for
1005 acceleration in fish development and the role of metamorphosis. J. Sea Res. 66,
1006 419–423. https://doi.org/10.1016/J.SEARES.2011.04.016
1007 Le Moullac, G., Soyez, C., Latchere, O., Vidal-Dupiol, J., Fremery, J., Saulnier, D.,
1008 Lo Yat, A., Belliard, C., Mazouni-Gaertner, N., Gueguen, Y., 2016. Pinctada
1009 margaritifera responses to temperature and pH: Acclimation capabilities and
1010 physiological limits. Estuar. Coast. Shelf Sci. 182, 261–269.
1011 https://doi.org/10.1016/j.ecss.2016.04.011
1012 Le Moullac, G., Tiapari, J., Teissier, H., Martinez, E., Cochard, J.-C., 2012. Growth

and gonad development of the tropical black-lip pearl oyster, Pinctada margaritifera (L.), in the Gambier archipelago (French Polynesia). Aquac. Int. 20, 305–315.
Lefebvre, S., Claquin, P., Orvain, F., Véron, B., Charpy, L., 2012. Spatial and temporal dynamics of size-structured photosynthetic parameters (PAM) and primary production (13C) of pico- and nano-phytoplankton in an atoll lagoon. Mar. Pollut. Bull. 65, 478–489. https://doi.org/10.1016/J.MARPOLBUL.2012.04.011
Linard, C., Gueguen, Y., Moriceau, J., Soyez, C., Hui, B., Raoux, A., Cuif, J.P., Cochard, J.-C., Le Pennec, M., Le Moullac, G., 2011. Calcein staining of calcified structures in pearl oyster Pinctada margaritifera and the effect of food resource level on shell growth. Aquaculture 313, 149–155. https://doi.org/10.1016/J.AQUACULTURE.2011.01.008
Long KY, C., Le Moullac, G., 2017. Shell Growth Performance of Hatchery Produced Pinctada margaritifera: Family Effect and Relation with Cultured Pearl Weight. J. Aquac. Res. Dev. 08, 1–6. https://doi.org/10.4172/2155-9546.1000480
Loret, P., Pastoureaud, A., Bacher, C., Delesalle, B., 2000. Phytoplankton composition and selective feeding of the pearl oyster Pinctada margaritifera in the Takapoto lagoon (Tuamotu Archipelago, French Polynesia):in situ study using optical microscopy and HPLC pigment analysis. Mar. Ecol. Prog. Ser. 199, 55–67. https://doi.org/10.3354/meps199055
Marques, G.M., Augustine, S., Lika, K., Pecquerie, L., Domingos, T., Kooijman, S.A.L.M., 2018. The AmP project: Comparing species on the basis of dynamic energy budget parameters. PLOS Comput. Biol. 14, e1006100. https://doi.org/10.1371/journal.pcbi.1006100
Molnár, P.K., Derocher, A.E., Klanjscek, T., Lewis, M.A., 2011. Predicting climate change impacts on polar bear litter size. Nat. Commun. 2, 186. https://doi.org/10.1038/ncomms1183
Muller, E.B., Lika, K., Nisbet, R.M., Schultz, I.R., Casas, J., Gergs, A., Murphy, C.A., Nacci, D., Watanabe, K.H., 2019. Regulation of reproductive processes with dynamic energy budgets. Funct. Ecol. https://doi.org/10.1111/1365-2435.13298
Pace, D.A., Marsh, A.G., Leong, P., Green, A., Hedgecock, D., Manahan, D.T., 2006. Physiological bases of genetically determined variation in growth of bivalve larvae (Crassostrea gigas). J. Shellfish Res. 25.
Pagano, M., Rodier, M., Guillaumot, C., Thomas, Y., Henry, K., Andréfouët, S., 2017. Ocean-lagoon water and plankton exchanges in a semi-closed pearl farming atoll lagoon (Ahe, Tuamotu archipelago, French Polynesia). Estuar. Coast. Shelf

Sci. 191, 60–73.
Philippart, C.J.M., Amaral, A., Asmus, R., van Bleijswijk, J., Bremner, J., Buchholz, F., Cabanellas-Reboredo, M., Catarino, D., Cattrijsse, A., Charles, F., Comtet, T., Cunha, A., Deudero, S., Duchêne, J.C., Fraschetti, S., Gentil, F., Gittenberger, A., Guizien, K., Gonçalves, J.M., Guarnieri, G., Hendriks, I., Hussel, B., Vieira, R.P., Reijnen, B.T., Sampaio, I., Serrao, E., Pinto, I.S., Thiebaut, E., Viard, F., Zuur, A.F., 2012. Spatial synchronies in the seasonal occurrence of larvae of oysters (Crassostrea gigas) and mussels (Mytilus edulis/galloprovincialis) in European coastal waters. Estuar. Coast. Shelf Sci. 108, 52–63. https://doi.org/10.1016/j.ecss.2012.05.014
Picoche, C., Le Gendre, R., Flye-Sainte-Marie, J., Françoise, S., Maheux, F., Simon, B., Gangnery, A., 2014. Towards the Determination of Mytilus edulis Food Preferences Using the Dynamic Energy Budget (DEB) Theory. PLoS One 9, e109796. https://doi.org/10.1371/journal.pone.0109796
Pouvreau, S., Bacher, C., Héral, M., 2000a. Ecophysiological model of growth and reproduction of the black pearl oyster, Pinctada margaritifera: Potential applications for pearl farming in French Polynesia. Aquaculture 186, 117–144. https://doi.org/10.1016/S0044-8486(99)00373-7
Pouvreau, S., Bodoy, A., Buestel, D., 2000b. In situ suspension feeding behaviour of the pearl oyster, Pinctada margaritifera: combined effects of body size and weather-related seston composition. Aquaculture 181, 91–113.
Pouvreau, S., Gangnery, A., Tiapari, J., Lagarde, F., Garnier, M., Bodoy, A., 2000c. Gametogenic cycle and reproductive effort of the tropical blacklip pearl oyster, Pinctada margaritifera (Bivalvia: Pteriidae), cultivated in Takapoto atoll (French Polynesia). Aquat. Living Resour. 13, 37–48.
Pouvreau, S., Prasil, V., 2001. Growth of the black-lip pearl oyster, Pinctada margaritifera, at nine culture sites of French Polynesia: synthesis of several sampling designs conducted between 1994 and 1999. Aquat. Living Resour. 14, 155–163.
Pouvreau, S., Tiapari, J., Gangnery, A., Lagarde, F., Garnier, M., Teissier, H., Haumani, G., Buestel, D., Bodoy, A., 2000d. Growth of the black-lip pearl oyster, Pinctada margaritifera, in suspended culture under hydrobiological conditions of Takapoto lagoon (French Polynesia). Aquaculture 184, 133–154.
Ruiz, C., Abad, M., Sedano, F., Garcia-Martin, L.O., López, J.L.S., 1992. Influence of seasonal environmental changes on the gamete production and biochemical composition of Crassostrea gigas (Thunberg) in suspended culture in El Grove, Galicia, Spain. J. Exp. Mar. Bio. Ecol. 155, 249–262.

1087 https://doi.org/10.1016/0022-0981(92)90066-J
1088 Sakka, A., Legendre, L., Gosselin, M., LeBlanc, B., Delesalle, B., Price, N., 1999.
1089 Nitrate, phosphate, and iron limitation of the phytoplankton assemblage in the
1090 lagoon of Takapoto Atoll (Tuamotu Archipelago, French Polynesia). Aquat.
1091 Microb. Ecol. 19, 149–161. https://doi.org/10.3354/ame019149
1092 Sangare, N., Lo-Yat, A., Le Moullac, G., Pecquerie, L., Thomas, Y., Beliaeff, B.,
1093 Andréfouët, S., 2019. Estimation of physical and physiological performances of
1094 blacklip pearl oyster larvae in view of DEB modeling and recruitment
1095 assessment. J. Exp. Mar. Bio. Ecol. 512, 42–50.
1096 https://doi.org/10.1016/J.JEMBE.2018.12.008
1097 Sauriau, P.-G., Kang, C.-K., 2000. Stable isotope evidence of benthic microalgae-
1098 based growth and secondary production in the suspension feeder
1099 Cerastoderma edule (Mollusca, Bivalvia) in the Marennes-Oléron Bay, in:
1100 Island, Ocean and Deep-Sea Biology. Springer Netherlands, Dordrecht, pp.
1101 317–329. https://doi.org/10.1007/978-94-017-1982-7_29
1102 Southgate, P., Lucas, J., 2011. The pearl oyster. Elsevier.
1103 Thomas, Y., Dumas, F., Andréfouët, S., 2016a. Larval connectivity of pearl oyster
1104 through biophysical modelling; evidence of food limitation and broodstock effect.
1105 Estuar. Coast. Shelf Sci. 182, 283–293.
1106 Thomas, Y., Dumas, F., Andréfouët, S., 2014. Larval dispersal modeling of pearl
1107 oyster pinctada margaritifera following realistic environmental and biological
1108 forcing in ahe atoll lagoon. PLoS One 9, e95050.
1109 https://doi.org/10.1371/journal.pone.0095050
1110 Thomas, Y., Garen, P., Bennett, A., Le Pennec, M., Clavier, J., 2012. Multi-scale
1111 distribution and dynamics of bivalve larvae in a deep atoll lagoon (Ahe, French
1112 Polynesia). Mar. Pollut. Bull. 65, 453–462.
1113 Thomas, Y., Garen, P., Courties, C., Charpy, L., 2010. Spatial and temporal
1114 variability of the pico-and nanophytoplankton and bacterioplankton in a deep
1115 Polynesian atoll lagoon. Aquat. Microb. Ecol. 59, 89–101.
1116 Thomas, Y., Garen, P., Pouvreau, S., 2011. Application of a bioenergetic growth
1117 model to larvae of the pearl oyster Pinctada margaritifera L. J. sea Res. 66,
1118 331–339.
1119 Thomas, Y., Pouvreau, S., Alunno-Bruscia, M., Barillé, L., Gohin, F., Bryère, P.,
1120 Gernez, P., 2016b. Global change and climate-driven invasion of the Pacific
1121 oyster (Crassostrea gigas) along European coasts: a bioenergetics modelling
1122 approach. J. Biogeogr. 43, 568–579.
1123 Torréton, J., Dufour, P., 1996. Temporal and spatial stability of bacterioplankton

biomass and productivity in an atoll lagoon. Aquat. Microb. Ecol. 11, 251–261. https://doi.org/10.3354/ame011251

van der Meer, J., 2006. An introduction to Dynamic Energy Budget (DEB) models with special emphasis on parameter estimation. J. Sea Res. 56, 85–102. https://doi.org/10.1016/J.SEARES.2006.03.001

Welschmeyer, N.A., 1994. Fluorometric analysis of chlorophyll a in the presence of chlorophyll b and pheopigments. Limnol. Oceanogr. 39, 1985–1992. https://doi.org/10.4319/lo.1994.39.8.1985